Journal of Magnetic Resonance **139,** 181–185 (1999)
Article ID jmre.1999.1785, available online at http://www.idealibrary.com on IDEAL®

Determination of $^3J(H3'_i, P_{i+1})$ and $^3J(H5'_i/5''_i, P_i)$ Coupling Constants in ^{13}C-Labeled Nucleic Acids Using Constant-Time HMQC

Weidong Hu,*,[1] Serge Bouaziz,*,† Eugene Skripkin,* and Abdelali Kettani*

*Cellular Biochemistry & Biophysics Program, Box 557, Memorial Sloan-Kettering Cancer Center, 1275 York Avenue, New York, New York 10021; and †Universite Rene Descartes, Laboratoire de Pharmacochimie Moleculaire et Structurale, URA 1500 CNRS, 4 Av. de l'Observatoire, 75270 Paris Cedex 06, France

Received December 2, 1998; revised April 7, 1999

A novel ^1H–^{13}C correlated two-dimensional experiment, CT-HMQC-*J*, for the measurement of three-bond proton–phosphorus coupling constants in ^{13}C-labeled DNA is described. The experiment is based on the intensity difference of ^1H–^{13}C cross peaks in the presence and absence of the proton–phosphorus coupling interaction during the constant-time period in HMQC experiment. The ^3J(H, P) coupling constants can be easily extracted from the intensity ratios of the two experiments. The method has been applied to a uniformly ^{13}C,^{15}N-labeled d(GGAGGAT) 7-mer DNA sample. The proton–phosphorus coupling constants determined from CT-HMQC-*J*, together with the other three-bond coupling constants, are used to determine β and ϵ torsion angles. The introduction of β and ϵ restraints has improved the convergence as well as the quality of d(GGAGGAT) structure.

Key Words: **CT-HMQC-*J*; nucleic acids; structure refinement; ^1H–^{31}P coupling constant; torsion angles.**

Backbone torsion angles of nucleic acids are an important resource for local structural determination because the proton–proton NOE can only provide constraints for γ and δ angles out of six backbone torsion angles (α to ζ). Torsion angles can be deduced from three-bond coupling constants using the Karplus equation. In order to obtain a unique torsion angle from the Karplus equation, three related coupling constants are needed due to the fact that multiple torsion angles correspond to a given coupling constant in the Karplus curve. Coupling constants of $^3J(H3'_i, P_{i+1})$ and $^3J(H5'_i/5''_i, P_i)$ are thus critical in obtaining unique $\beta(P_i$–$O5'_i$–$C5'_i$–$C4'_i)$ and $\epsilon(C4'_i$–$C3'_i$–$O3'_i$–$P_{i+1})$ angles. Some methods have been developed to measure the $^3J(H3'_i, P_{i+1})$ and $^3J(H5'_i/5''_i, P_i)$ coupling constants for ^{13}C-unlabeled and uniformly ^{13}C-labeled nucleic acids (*1–4*). In this report, we present a different, yet a straightforward, approach to measure the $^3J(H3'_i, P_{i+1})$ and $^3J(H5'_i/5''_i, P_i)$ coupling constants. The proposed experiment, CT-HMQC-*J*, uses the principle developed in the $^3J(H_N$–$H_\alpha)$ coupling measurement (*5*) and HSQC spin echo difference experiment (*6*).

[1] To whom correspondence should be addressed. Fax: (212) 717-3066. E-mail: weidong@sbnmr1.ski.mskcc.org.

The values of ^3J(H, P) coupling constants can be extracted easily from the intensity ratios of two 2D experiments with and without ^3J(H, P) dephasing. Its utility is demonstrated for a uniformly ^{13}C,^{15}N-labeled d(GGAGGAT) 7-mer DNA duplex sample.

The pulse sequences of CT-HMQC-*J* are illustrated in Fig. 1. The experiments are modified from the constant-time HMQC scheme (*7*). Two pulse sequences, reference and attenuated experiments, are used to determine the $^3J(H3'_i, P_{i+1})$ and $^3J(H5'_i/5''_i, P_i)$ coupling constants. The shaded proton scramble pulse is used to destroy proton antiphase coherence developed during the constant-time period due to the proton homonuclear coupling interaction. The constant time duration, T_c, is set to 25 ms so that the dephasing of ^{13}C magnetization due to ^{13}C–^{13}C one-bond coupling constant (~40 Hz) is eliminated. The 180° pulses on ^{31}P in the T_c period are applied in such a way that the coupling interaction between ^1H and ^{31}P is refocused in the reference and active in the attenuated experiments. The composite 180° pulses on ^{31}P in the attenuated experiment are used to remove potential error caused by different total length of ^{31}P pulses from the two experiments. The dephasing factor in the attenuated experiment is dependent upon the duration of constant time and the ^3J(H, P) coupling constant. Since coupling interaction between ^{13}C and ^{31}P is refocused in the two experiments, the attenuated factor is $\cos(\pi JT_c)$, where the J is ^3J(H, P) coupling constant. Thus, the ^3J(H, P) coupling constant is given by equation

$$^3J(\mathrm{H, P}) = \arccos(I_{\mathrm{att}}/I_{\mathrm{ref}})/(\pi T_c), \qquad [1]$$

where the I_{att} and I_{ref} are the volumes of cross peaks from the attenuated and reference experiments.

The implementation of the CT-HMQC-*J* experiment has been demonstrated on 1.5 mM uniformly ^{13}C,^{15}N-labeled d(GGAGGAT) DNA oligonucleotide (*8*) recorded in D_2O on a Varian Inova 500-MHz spectrometer at 0°C. The experiments were processed and analyzed using FELIX 97.0 (Molecular Simulations) on a SGI O2 workstation. Shown in Fig. 2A is the region of $^1H3'$–$^{13}C3'$ and $^1H5'/H5''$–$^{13}C5'$ from the reference

1090-7807/99 $30.00

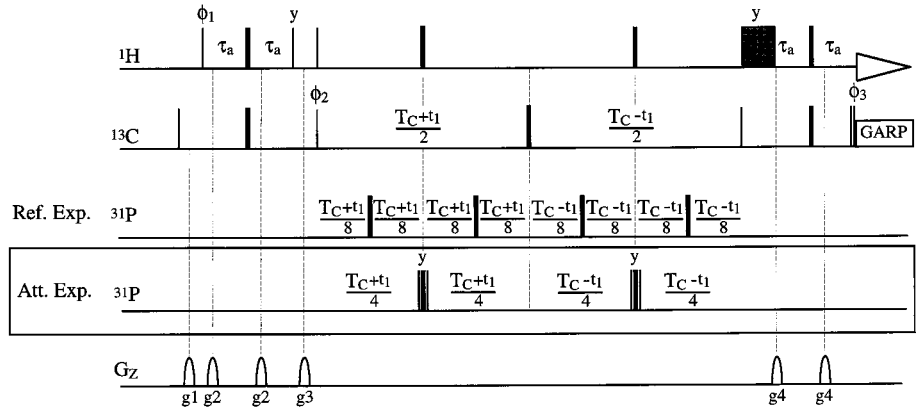

FIG. 1. Pulse sequences of the CT-HMQC-*J* experiment for ^3J(H, P) measurement in a ^{13}C-labeled oligonucleotide. The experiment is composed of reference and attenuated schemes. Narrow and wide bars correspond to 90° and 180° pulses, respectively. The shaded square is a proton scramble pulse with duration of 1 ms and strenth of 30.5 kHz. The phases of all pulses are x axis unless otherwise indicated. The ^{1}H, ^{13}C, and ^{31}P carrier frequencies were 5.05, 75, and −4.5 ppm, respectively. Field strengths of the ^{1}H pulse, ^{13}C high-power pulse, GARP decoupling (*18*) on ^{13}C, and ^{31}P hard pulse were 30.5, 20.8, 2.2, and 7.4 kHz, respectively in both reference and attenuated experiments. Strengths and duration of gradients were g1 = (11 G/cm, 0.5 ms), g2 = (9 G/cm, 0.3 ms), g3 = (28 G/cm, 1 ms), g4 = (9 G/cm, 0.2 ms). Constant time duration and τ_a were set to 25 and 1.5 ms, respectively. Phase cycling was $\phi_1 = x, -x$; $\phi_2 = x, x, -x, -x$; $\phi_3 = 4(x), 4(-x)$; and Acq. = $x, -x, -x, x$. Quadrature detection during t_1 was achieved via States–TPPI (*19*) on ϕ_2.

experiment scheme. The resonance assignments of ^{1}H and ^{13}C have been given by Kettani *et al.* (*8*). The stereospecific assignments of H5′(proS) and H5″(proR) have been achieved from both the 2D HCCH-E.COSY (*9*) and the HSQC-C5′H5′ experiments (*10*). Peak intensity comparisons from the reference and attenuated experiments are illustrated in Figs. 2B and 2C, the 1D slices from CT-HMQC-*J* spectra for the ^{1}H3′–^{13}C3′ and ^{1}H5′/H5″–^{13}C5′ of A3 ribose, respectively. The derived $^3J(H3'_i, P_{i+1})$ and $^3J(H5'_i/5''_i, P_i)$ coupling constants using Eq. [1] are listed in Table 1. The error of the experiment has been estimated by assuming the coupling constant of ^{1}H1′–^{31}P to be zero as described by Legault *et al.* (*11*). The root-mean-square deviation of relative volume based on all H1′–C1′ cross peaks is 0.005. Since this deviation only counts for 0.4 ~ 0.6% of the volume ratio of H3′–C3′ and H5′/H5″–C5′, this error is not further considered in deriving β and ϵ angles from the $^3J(H3'_i, P_{i+1})$ and $^3J(H5'_i/5''_i, P_i)$ coupling constants.

For a two-spin system in a large biomolecule, the multiple-quantum coherence relaxes more slowly than the corresponding single-quantum magnetization state (*12*). Therefore, compared to the CT-HSQC, the CT-HMQC enhances the intensity of ^{1}H–^{13}C cross peaks of ribose in a 36-mer RNA sample by two- to threefold except for ^{1}H5′/H5″–^{13}C5′, whose multiple-quantum relaxation rate is increased by the dipole interaction from the geminal proton (*13*). Although the cross peaks of ^{1}H5′/H5″–^{13}C5′ are weaker than those of ^{1}H3′–^{13}C3′ in this study, decent intensity of ^{1}H5′/H5″–^{13}C5′ cross peaks from a moderately sized RNA (27-mer) has been observed (unpublished result). The intensity of ^{1}H5′/H5″–^{13}C5′ cross peak can be enhanced by the CT-HTQC scheme (*13*); unfortunately, it cannot be used to measure the $^3J(H5'_i/5''_i, P_i)$ coupling constant because the magnetization of both protons is transverse during the constant-time period.

In addition to the $^3J(H5'_i/5''_i, P_i)$ and $^3J(H3'_i, P_{i+1})$, other couplings required for a unique β and ϵ angle ($^3J(C4'_i, P_i)$,

TABLE 1
Coupling Constants and Backbone Torsion Angles of d(GGAGGAT)

	G1	G2	A3	G4	G5	A6	T7
$^3J(P, C_{4'})$ (Hz)		11.0	8.6	6.0	8.4	7.9	10.2
$^3J(P, H_{5'})$ (Hz)		0.7	2.3	2.1	0.8	2.4	1.6
$^3J(P, H_{5''})$ (Hz)		2.9	3.5	1.3	0.3	4.8	1.8
β(°)/rms$J$[a]		173/0.6	168/1.9	190/3.4	182/2.4	155/1.9	179/1.0
$^3J(C_{4'}, P)$ (Hz)	12.3	6.5	ca. 0	8.3	7.0	8.4	
$^3J(H_{3'}, P)$ (Hz)	2.5	7.7	8.2	3.9	6.5	8.6	
$^3J(C_{2'}, P)$ (Hz)	1.5	1.5	8.2	0.9	ca. 0	1.3	
ϵ(°)/rms$J$	180/0.5	221/1.1	266/0.6	198/1.8	213/1.5	217/0.2	

[a] rms$J$ is calculated using Eq. [2].

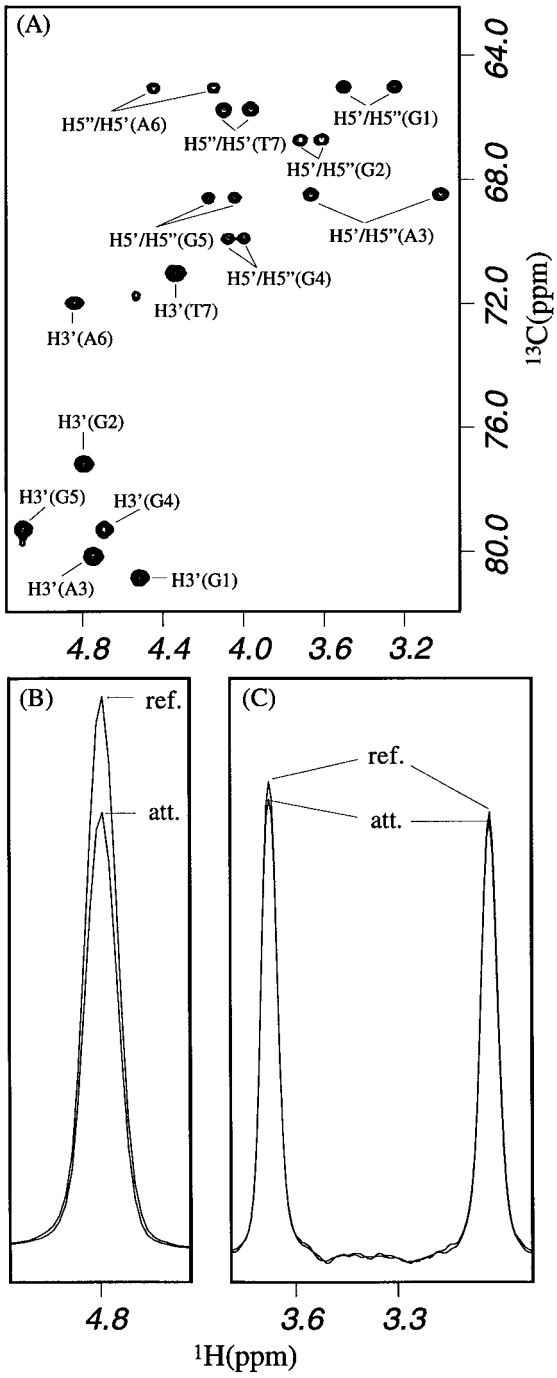

FIG. 2. Shown in (A) is the spectrum of the CT-HMQC-*J* reference experiment for the region of H3′–C3′ and H5′/H5″–C5′ of the ^{13}C-labeled d(GGAGGAT) oligonucleotide. The spectral widths(Hz)/complex points along F1, F2 were 4400/80 and 8000/1024 with 160 transients per FID. The total experimental time was 8.5 h. The F1 resolution was enhanced through mirror-image linear prediction (*20*) resulting in a final matrix size of 256 × 2048 real points. The H5′ and H5″ are corresponding to proS and proR, respectively. Shown in (B) is the peak intensity comparison from reference (ref.) and attenuated (att.) experiments for ^{1}H3′–^{13}C3′ of A3 ribose sliced at ^{13}C chemical shift of 80.2 ppm. Shown in (C) is the peak intensity comparison from reference (ref.) and attenuated (att.) experiments for ^{1}H5′/H5″–^{13}C5′ of A3 ribose sliced at ^{13}C chemical shift of 68.5 ppm. The 1D slices from ref. and att. experiments are scaled to the same noise level in both (A) and (B).

$^{3}J(C4'_i, P_{i+1})$, and $^{3}J(C2'_i, P_{i+1})$) have been determined from quantitative HCP (*14*) and HSQC-*J* (*11*) experiments and are listed in Table 1. The most favorable value of torsion angle can thus be found from the three related couplings using the equation (*14*)

$$\text{rms}J = (\Sigma((J_{\text{exp}} - J_{\text{the}})^2)/3)^{1/2}, \qquad [2]$$

where the rms*J* is the root-mean-square deviation of the coupling constant, J_{exp} is the experimental coupling constant, and J_{the} is the calculated one from the parameterized Karplus equations (*15*) for a given value of a torsion angle. From the curves of rms*J* versus β and ϵ angles as shown in Fig. 3, the most favorable β and ϵ values are those which give the minimum rms*J* values. The deduced torsion angles and the associated rmsJ values are listed in Table 1.

The structure of the d(GGAGGAT) duplex DNA has been solved previously in our laboratory from a combined NMR–molecular dynamics study without any torsion angle restraints (*8*). The oligomer containing a tandem of the GGA triplet repeat sequence adopts a duplex structure where interlocked arrowhead-shaped motifs are aligned through A · A and G · G mismatch formation. The chain reversal in the p–A3–p segment is revealed by an unusual ϵ angle of A3, which has an averaged value of 277° from 15 refined structures (*8*). The ϵ angle of A3 has been determined to be 266° from this study, which verified the unusual value of this angle reported before (*8*).

To evaluate the effect of β and ϵ restraints on the structure of d(GGAGGAT) duplex, the structure calculation has been performed using the X-PLOR program (*16*). In the first stage, 15 structures of 100 attempts at embedding and optimization have been selected using distance geometry and simulated annealing refinement based on their acceptable covalent geometry, low distance restraints violations, and favorable nonbonded energy. In the second stage, these 15 structures have been submitted to molecular dynamics refinement with and without β and ϵ restraints. The range of the β and ϵ has been set to $\pm$30° about the values in Table 1.

The quality of the two sets of 15 structures obtained with and without β and ϵ restraints has been measured. The use of β and ϵ angles increases the convergence of the structures. Compared to the structures without β and ϵ restraints, the pairwise rmsd is reduced from 0.94 $\pm$ 0.28 Å to 0.69 $\pm$ 0.33 Å, and the rmsd from the mean structure is reduced from 0.65 $\pm$ 0.22 Å to 0.47 $\pm$ 0.22 Å. At the same time, the quality of the structures using the β and ϵ restraints is better. This is evidenced by the improved rmsd for the distance restraints, the rmsd is reduced from 0.017–0.021 to 0.015–0.02 Å. No distance violation (>0.2 Å) has been observed for both cases.

In summary, we have introduced a 2D experiment, CT-HMQC-*J*, to determine the $^{3}J(H3'_i, P_{i+1})$ and $^{3}J(H5'_i/5''_i, P_i)$ coupling constants in a straightforward manner for ^{13}C-labeled

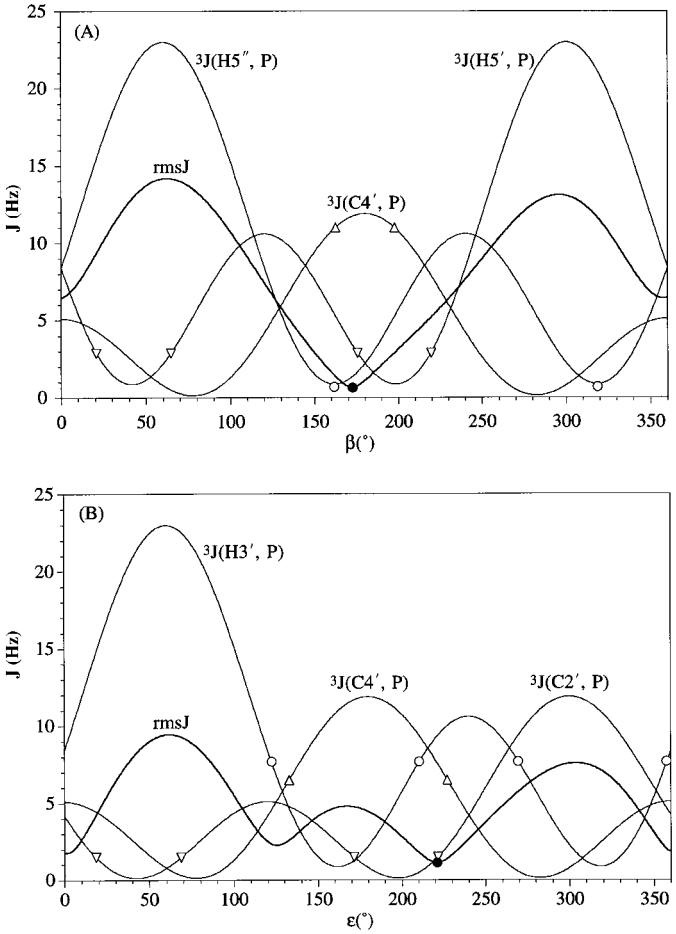

FIG. 3. Coupling constants versus β (A) and ϵ (B) torsion angles of residue G2: Thin solid lines in (A) are the theoretical Karplus curves of $^3J(H5''_i, P_i)$, $^3J(H5'_i, P_i)$, $^3J(C4'_i, P_i)$ based on the parameterized Karplus equations (*15*) and the thicker solid line is the rms*J* curve calculated using Eq. [2]. The experimental coupling constants of $^3J(H5''_i, P_i)$, $^3J(H5'_i, P_i)$, $^3J(C4'_i, P_i)$, and the minimum rms*J* are represented by ○, ▽, △, and ●, respectively. Thin solid lines in (B) are the theoretical Karplus curves of $^3J(H3'_i, P_{i+1})$, $^3J(C2'_i, P_{i+1})$, and $^3J(C4'_i, P_i)$ and the thicker solid line is the rms*J* curve calculated using Eq. [2]. The experimental coupling constants of $^3J(H3'_i, P_{i+1})$, $^3J(C2'_i, P_{i+1})$, $^3J(C4'_i, P_{i+1})$, and the minimum rmsJ are represented by ○, ▽, △, and ●, respectively. The most favorable torsion angles are the ones corresponding to the minimum values of rms*J* in (A) and (B).

DNA. The method is applicable to moderately sized ^{13}C-labeled RNA (unpublished results). To resolve the chemical shift overlaps for a larger nucleotide sample, the 2D experiment can be extended to a 3D version using a ^{13}C-TOCSY transfer step so that the ^{1}H3′–^{13}C3′ and ^{1}H5′/H5″–^{13}C5′ cross peaks can be read out from the well-resolved ^{1}H1′ region. A similar approach, a 3D HCCH-COSY spin-echo difference experiment, has been reported recently to measure ^3J(C2′, P) (*17*). The β and ϵ angles deduced from $^3J(H3'_i, P_{i+1})$ and $^3J(H5'_i/5''_i, P_i)$ and other related coupling constants have improved the quality of the d(GGAGGAT) structure significantly.

ACKNOWLEDGMENTS

This work was supported under NIH Grant GM34504 to Dinshaw J. Patel. We thank D.J.P. for his encouragement and discussions during the course of this research.

REFERENCES

1. V. Sklenar and A. Bax, Measurement of ^{1}H–^{31}P NMR coupling constants in double-stranded DNA fragments, *J. Am. Chem. Soc.* **109,** 7525–7526 (1987).
2. H. Schwalbe, W. Samstag, J. W. Engels, W. Bermel, and C. Griesinger, Determination of ^3J(C,P) and ^3J(H,P) coupling constants in nucleotide oligomers with FIDS-HSQC, *J. Biomol. NMR* **3,** 479–486 (1993).
3. H. Schwalbe, J. P. Marino, G. C. King, R. Wechselberger, W. Bermel, and C. Griesinger, Determination of a complete set of coupling constants in ^{13}C-labeled oligonucleotides, *J. Biomol. NMR* **4,** 631–644 (1994).
4. G. M. Clore, E. C. Murphy, A. M. Gronenborn, and A. Bax, Determination of three-bond ^{1}H3′–^{31}P couplings in nucleic acids and protein–nucleic acid complexes by quantitative J correlation spectroscopy, *J. Magn. Reson.* **134,** 164–267 (1998).
5. H. Ponstingl and G. Otting, Rapid measurement of scalar three-bond ^{1}HN–$^1H_\alpha$ spin coupling constants in ^{15}N-labelled proteins, *J. Biomol. NMR* **12,** 319–324 (1998).
6. G. W. Vuister, A. C. Wang, and A. Bax, Measurement of three-bond nitrogen-carbon *J* couplings in protein uniformly enriched in ^{15}N and ^{13}C, *J. Am. Chem. Soc.* **115,** 5334–5335 (1993).
7. H. Kuboniwa, S. Grzesiek, F. Delaglio, and A. Bax, Measurement of H_N–H_α *J* couplings in calcium-free calmodium using new 2D and 3D water-flip-back methods, *J. Biomol. NMR* **4,** 871–878 (1994).
8. A. Kettani, S. Bouaziz, E. Skripkin, A. Majumdar, W. Wang, R. A. Jones, and D. J. Patel, The arrowhead DNA motif: $(G–G–A)_2$ triplet repeat sequence in low salt adopts a V-shaped interlocked mismatch-aligned duplex, *Structure,* in press (1999).
9. C. Griesinger and U. Eggenberger, Determination of proton–proton coupling constants in ^{13}C-labeled molecules, *J. Magn. Reson.* **97,** 426–434 (1992).
10. J. P. Marino, H. Schwalbe, S. J. Glaser, and C. Griesinger, Determination of γ and stereospecific assignment of H5′ protons by measurement of ^2J and ^3J coupling constants in uniformly ^{13}C labeled RNA, *J. Am. Chem. Soc.* **118,** 4388–4395 (1996).
11. P. Legault, F. M. Jucker, and A. Pardi, Improved measurement of ^{13}C, ^{31}P *J* coupling constants in isotopically labeled RNA, *FEBS Lett.* **362,** 156–160 (1995).
12. S. Grzesiek and A. Bax, Spin-locked multiple quantum coherence for signal enhancement in heteronuclear multidimensional NMR experiments, *J. Biol. NMR* **6,** 335–339 (1995).
13. J. P. Marino, J. L. Diener, P. B. Moore, and C. Griesinger, Multiple-quantum coherence dramatically enhances the sensitivity of CH and CH_2 correlations in uniformly ^{13}C-labeled RNA, *J. Am. Chem. Soc.* **119,** 7361–7366 (1997).
14. C. Richter, B. Reif, K. Wörner, S. Quant, J. P. Marino, J. W. Engels, C. Griesinger, and H. Schwalbe, A new experiment for the measurement of ^nJ(C, P) coupling constants including $^3J(C4'_i, P_i)$ and $^3J(C4'_i, P_{i+1})$ in oligonucleotides, *J. Biomol. NMR* **12,** 223–230 (1998).
15. M. M. W. Mooren, S. S. Wijmenga, G. A. van der Marel, J. H. van Boom, and C. W. Hilbers, The solution structure of the circular

trinucleotide cr($G_pG_pG_p$) determined by NMR and molecular mechanics calculation, *Nucleic Acids Res.* **13,** 164–167 (1994).

16. A. T. Brünger, "X-PLOR. A System for X-Ray Crystallography and NMR," Yale Univ. Press, New Haven, CT (1992).

17. C. G. Hoogstraten and A. Pardi, Measurement of carbon–phosphorus *J* coupling constants in RNA using spin-echo difference constant-time HCCH–COSY, *J. Magn. Reson.* **133,** 236–240 (1998).

18. A. J. Shaka, P. B. Barker, and R. Freeman, Computer-optimized decoupling scheme for wideband applications and low-level operation, *J. Magn. Reson.* **64,** 547–552 (1985).

19. D. Marion, M. Ikura, R. Tschudin, and A. Bax, Rapid recording of 2D NMR spectra without phase cycling. Application to the study of hydrogen exchange in proteins, *J. Magn. Reson.* **85,** 393–399 (1989).

20. G. Zhu and A. Bax, Improved linear prediction for truncated signals of known phase, *J. Magn. Reson.* **90,** 405–410 (1990).